Mechanism of Translocation and Kinetics of DNA Unwinding by the Helicase RecG†

Maria M. Martinez-Senac and Martin R. Webb*

MRC National Institute for Medical Research, Mill Hill, London NW7 1AA, United Kingdom

Received July 5, 2005; Revised Manuscript Received October 14, 2005

ABSTRACT: RecG is a DNA helicase involved in the repair of damage at a replication fork and catalyzes the reversal of the fork to a point beyond the damage in the template strand. It unwinds duplex DNA in reactions that are coupled to ATP hydrolysis. The kinetic mechanism of duplex DNA unwinding by RecG was analyzed using a quantitative fluorescence assay based on the process of contact quenching between Cy3 and Dabcyl groups attached to synthetic three-way DNA junctions. The data show that the protein moves at a rate of 26 bp s^{-1} along the duplex DNA during the unwinding process. RecG ATPase activity during translocation indicates a constant rate of 7.6 s^{-1}, measured using a fluorescent phosphate sensor, MDCC-PBP. These two rates imply a movement of ~3 bp per ATP hydrolyzed. We demonstrate in several trapping experiments that RecG remains attached to DNA after translocation to the end of the arm of the synthetic DNA junction. ATPase activity continues after translocation is complete. Dissociation of RecG from the product DNA occurs only very slowly, suggesting strong interactions between them. The data support the idea that interactions of the duplex template arm with the protein are the major sites of binding and production of translocation.

Helicases are enzymes with essential roles in a variety of fundamental DNA and RNA metabolic processes, including DNA replication, repair, recombination, transcription, and translation. They are molecular motors that use the chemical energy of nucleoside triphosphate hydrolysis, generally ATP, to drive the mechanical action of nucleic acid strand separation and translocation of the helicase along DNA for processive unwinding (*1*, *2*).

Here, we describe work on a bacterial helicase, RecG, that is involved in repair of damage at a replication fork. Under normal growth conditions, the bacterial DNA replication apparatus frequently meets various barriers in the form of DNA damage, secondary structure, or protein−DNA complexes that impede their progress prior to completion of chromosomal replication. If the replication fork stalls, the replisome disassembles and the fork is driven backward to form a four-way (Holliday) junction to restart replication. RecG is a superfamily 2 (SF-2)[1] helicase that catalyzes the reversal of the fork to a point beyond the damage in the template strand (*3*, *4*). This reversal reaction constitutes a major pathway for replication restart and allows priming of leading strand replication by template switching. The Holliday junction formed by this process may then migrate, for example, by the action of RuvAB, to re-establish the replication fork with the DNA lesion bypassed for later repair.

Insight into how RecG is able to catalyze the fork reversal has come from the crystal structure of *Thermotoga maritima* RecG in complex with an analogue of a stalled replication fork (*5*). This complex mimics the intermediate formed if synthesis terminates on the leading strand before that of the lagging strand. This type of structure is likely to occur if the polymerase reaches a base lesion on the leading strand template (*3*). Forks with a single-stranded leading arm have been shown to be the preferred substrate for RecG in vitro (*6*), but stalled replication forks in general may contain a wide variety of local DNA structures. RecG has well-conserved helicase domains linked to an N-terminal "wedge" domain that lies between the two forks and so provides specificity for binding a three-way branched DNA structure. It has been proposed that the helicase motor acts on the dsDNA portion of the junction, producing translocation by pulling the parental strands of a replication fork structure through two separate channels flanking the wedge domain (*5*). Neither of these channels is wide enough to accommodate dsDNA, so the second strands of each fork are stripped away. The wedge is essential for strong binding and efficient activity (*7*).

Structural data from members of helicase SF-2 suggest that nucleic acid binding occurs in a non-sequence-specific manner via the phosphodiester backbone. Such data indicate that SF-2 helicases can bind to both double- and single-stranded nucleic acids. Nevertheless, RecG appears to translocate along a duplex, as its main function is to catalyze the movement of a branch point along a dsDNA molecule (*1*). RecG shows ATPase activity is highly dependent upon dsDNA (*8*).

A complete understanding of the molecular mechanism by which this protein functions requires quantitative kinetic

† This work was supported by the Medical Research Council, U.K.

* To whom correspondence should be addressed. Telephone: (+44) 20 8816 2078. Fax: (+44) 20 8906 4477. E-mail: mwebb@nimr.mrc.ac.uk.

[1] Abbreviations: SF-2, superfamily 2; TAMRA, 5-tetramethylrhodamine; Db, Dabcyl; MDCC-PBP, phosphate binding protein modified at Cys197 with *N*-[2-(1-maleimidyl)ethyl]-7-(diethylamino)-coumarin-3-carboxamide; ssDNA, single-stranded DNA; dsDNA, double-stranded DNA.

10.1021/bi0512851 CCC: $30.25
Published on Web 11/30/2005

information about the intermediate steps involved in the translocation and unwinding processes. DNA unwinding by a processive helicase must involve the movement of the enzyme along a number of base pairs that are unwound during each cycle of ATP hydrolysis. Such a single unwinding step is termed the step size and may be one or several base pairs, reflecting specific features of the mechanism. The movement is repeated several or many times before the dissociation of the helicase from DNA. Processivity, the average number of steps prior to dissociation, varies considerably between helicases and may also vary with the reaction conditions.

The kinetic behavior of helicases has often been studied using "all or none" assays that detect only the final product or step of the reaction (i.e., completely unwound single-stranded DNA). However, a quantitative analysis of the dependence of the single-turnover time courses of DNA unwinding on duplex DNA length can yield estimates of the unwinding rate and the kinetic step size. These assays have involved the use of nucleic acids labeled either with a radioactive tag (*9*−*15*) or by a fluorescence probe (*16*−*20*) to monitor complete unwinding of the DNA.

This work reports the relationship between DNA translocation, unwinding, and ATP hydrolysis by RecG in an effort to understand how this DNA helicase fulfils its specific role in DNA repair. We have analyzed the kinetic mechanism of *T. maritima* RecG using a quantitative fluorescence assay to monitor RecG helicase-catalyzed unwinding of duplex DNA in real time. This assay is based on the process of static quenching between a fluorophore and a quencher placed in an adjacent position at the ends of a duplex DNA. The quenching is relieved on physical separation of the two strands. The kinetics of ATP hydrolysis by RecG helicase have also been measured in the presence of a DNA substrate. Release of inorganic phosphate (P_i) from RecG was monitored with a P_i sensor, a fluorescent coumarin-labeled phosphate binding protein (MDCC-PBP) (*21*). The P_i from each turnover of ATP hydrolysis can be observed before and after the steady state is achieved and therefore gives a measure of ATPase activity in real time.

These measurements were performed in the absence and presence of a protein trap, such as heparin or unlabeled DNA. Such traps have been used widely to ensure that the helicase dissociated from the DNA or initially free in the solution is prevented from rebinding to the original DNA (*9*, *11*, *12*, *22*−*24*). In this way, each prebound helicase is involved in only a single round of DNA unwinding: reactions are single-turnover with respect to the DNA, although multiple rounds of ATP hydrolysis can occur.

EXPERIMENTAL PROCEDURES

Protein Preparation. MDCC-PBP (*21*, *25*) and RecG helicase (*5*) were prepared as described previously. The *T. maritima* RecG expression system was kindly provided by D. B. Wigley (Cancer Research UK). RecG concentrations were determined spectrophotometrically using an extinction coefficient of 57 560 M^{-1} cm^{-1} at 280 nm, calculated using ProtParam, a sequence analysis tool of the ExPASy Proteomics Server of the Swiss Institute of Bioinformatics (SIB) (*26*).

DNA Preparation. The DNA substrates that were employed were two-way and three-way forks. The constituent oligonucleotides were synthesized and HPLC-purified by Eurogentec S.A. Fluorescently labeled oligonucleotides were supplied and HPLC-purified by MWG Biotech AG. The oligonucleotides were concentrated to ~1.5 mM in H_2O and annealed at a molar ratio of 1:1:1 in a buffer of 50 mM PIPES (pH 6.3) and 200 mM KCl (~200 μL). The annealing program comprised an initial denaturing step of 1 min at 95 °C, and then consecutive linear changes to 70 °C over 10 min, to 50 °C over 40 min, to 20 °C over 10 min, and finally to 4 °C over 10 min. The annealed substrate was purified on a Superdex 200 HR 10/30 column (Amersham Biosciences) equilibrated in 50 mM PIPES (pH 6.3) and 200 mM KCl. The purified junctions were desalted on a NAP 25 column (Amersham Biosciences) in H_2O and vacuum concentrated to ~1.5 mM.

DNA Binding Assays. These were performed using a three-way DNA junction labeled with the fluorophore Cy3 at the 5′-end of the duplex in the template arm. The oligonucleotides were 5′-TTAGTTGTTCGTAGTGCTCGTCTGGCTCTG-3′, 5′-Cy3-CAGAGCCAGAATCATAGCCATAACACGATC-3′, and 5′-GAGCACTACGAACAACTAA-3′. The measurements were performed in buffer A [50 mM Tris·acetate (pH 8.0), 20 mM potassium acetate, 1 mM dithiothreitol, and 0.7 mM magnesium acetate] at 20 °C using a Hi-Tech SF61 DX2 stopped-flow instrument equipped with a Xe−Hg lamp and with 4 mm slits for the excitation light at 548 nm, and Cy3 fluorescence emission was monitored using a 570 nm cutoff filter. RecG at different concentrations (from 120 to 600 nM) was rapidly mixed with 60 nM three-way junction. All concentrations quoted for stopped-flow measurements are the final ones after mixing.

Equilibrium binding titrations were carried out in a Perkin-Elmer LS50B fluorimeter with a xenon lamp. The same DNA junction described above (60 nM) in buffer A at 20 °C was excited at 548 nm, and emission spectra were collected after addition of different concentrations of RecG protein (from 83 to 522 nM). The data were fitted to a quadratic equation taking into account that a significant proportion of the DNA is bound to the protein.

Steady-State ATPase Activity Measurements. Fluorescence measurements were taken in a Perkin-Elmer LS50B fluorimeter with a xenon lamp. Excitation and emission wavelengths were 436 and 455 nm, respectively, with excitation and emission slit widths of 2.5 nm. ATPase activity was measured by linking ATP hydrolysis to the change in fluorescence observed in the P_i sensor MDCC-PBP (*21*). Reactions were carried out with 10 nM RecG at various concentrations of ATP in a solution containing 1.25 μM bovine serum albumin, 50 nM DNA junction, and 20 μM MDCC-PBP in buffer A at 20 °C. In calculations of ATP turnover, it is assumed that all of the enzyme preparation is active. The fluorescence signal of MDCC-PBP was calibrated using known concentrations of a P_i standard. These results showed that the values of K_m and k_{cat} for ATP are 42 μM and 5.2 s^{-1}, respectively. Other measurements were taken at 200 μM ATP unless otherwise stated: this concentration is close to saturating under the conditions that were employed.

Pre-Steady-State ATPase Activity Measurements. Pre-steady-state measurements were carried out using a stopped-flow instrument as described above with a monochromator with 436 nm excitation and a 455 nm cutoff filter for the

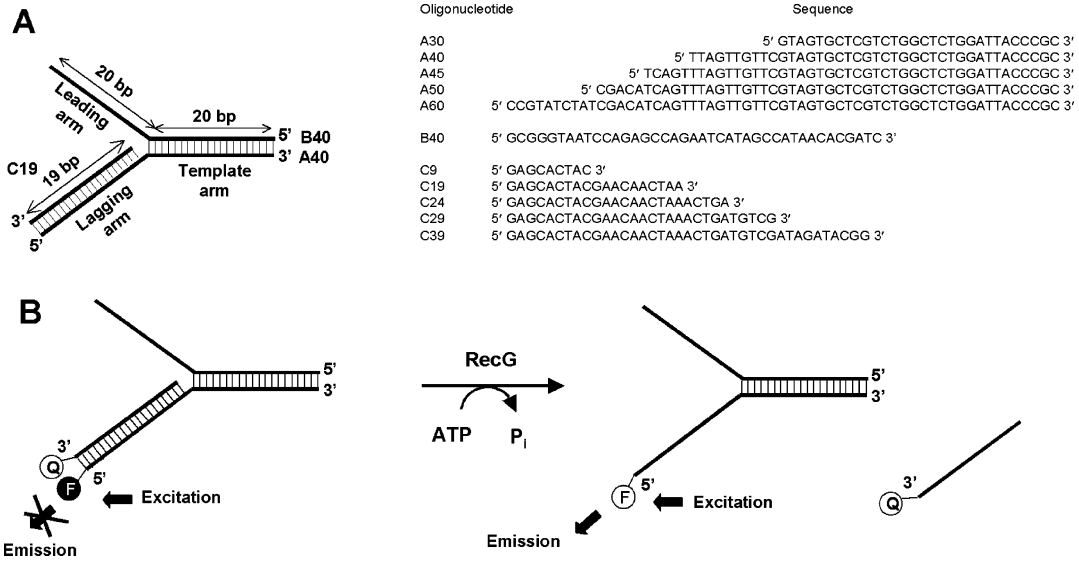

FIGURE 1: Schematic representation of the DNA substrate used in the translocation and unwinding experiments and of the basis of the fluorescent translocation assay. (A) Example of the three-way DNA junction substrates used in our studies, made from annealing the three separate oligonucleotides of different lengths (A40, B40, and C19). Sequences are in the table. Each three-way DNA junction consists of a 20 bp duplex template arm ahead of the fork, a single-base gap at the junction on the lagging arm followed by 9, 19, 24, 29, or 39 bp of duplex DNA, and a 20-base single-stranded leading arm. The DNA substrates differ only in the length of the duplex lagging arm of the junction and are called A30−B40−C9, A40−B40−C19, A45−B40−C24, A50−B40−C29, and A60−B40−C39. (B) The DNA substrates used for the unwinding reaction assays are labeled at the 5′-end of oligonucleotide A with the fluorophore (F) and at the 3′-end of oligonucleotide C with the quencher (Q). When in proximity, Q quenches the fluorescence emission of F. After unwinding, the quencher should separate from the fluorophore, allowing emission from the latter.

emission. Concentrations were as follows: 5 nM RecG, 100 nM DNA junction, 5 μM MDCC-PBP, and 200 μM ATP in buffer A at 20 °C. A P_i mop was used throughout to ensure that MDCC-PBP was P_i-free immediately prior to the measurements. The P_i mop consisted of 0.01 unit/mL bacterial purine nucleoside phosphorylase (Sigma) and 200 μM 7-methylguanosine which sequester P_i chemically as ribose 1-phosphate. The fluorescence signal of MDCC-PBP was calibrated using a P_i standard.

DNA Unwinding Measurements. The experiments were performed in buffer A at 20 °C using a Hi-Tech SF61 DX2 stopped-flow instrument equipped with a Xe−Hg lamp and with 4 mm slits for the excitation light. For the fluorophore Cy3−quencher Dabcyl (Db) experiments, the Cy3 was excited at 548 nm and its fluorescence emission was monitored using a 570 nm cutoff filter. The preformed DNA−RecG complex was allowed to equilibrate for 5 min, and the reaction was initiated by rapid mixing with a solution containing ATP. All concentrations quoted are the final ones after mixing and were as follows: 60 nM RecG, 30 nM DNA junction, and 200 μM ATP.

Analysis of Kinetic Data. Kinetic simulations were performed using ModelMaker (version 3, Cherwell Scientific, Oxford, U.K.). Kinetic data were fitted to theoretical curves using either Sigmaplot (version 8, Systat Software Inc., Richmond, CA) or Grafit (*27*).

RESULTS

DNA Substrate Design. The three-way DNA junctions in our kinetic studies were composed of three separate oligonucleotides of different lengths, and an example is depicted schematically in Figure 1A. The oligonucleotide sequences were chosen in an effort to prevent the formation of secondary structure or incorrect hybridization during the course of annealing. Each DNA junction structure consists of a 20 bp duplex template arm ahead of the fork, a single base gap at the junction on the lagging arm followed by 9, 19, 24, 29, or 39 bp of duplex, and a 20-base single-stranded leading arm. These DNA substrates differ only in the length of the duplex lagging arm of the junction. The designs were based on those used in the crystallographic studies of the protein (*5*). Two-way DNA junctions were used in some studies, and here the lagging arm was single-stranded instead of duplex.

Kinetic Analysis of the Double-Stranded DNA Unwinding by RecG. Most measurements were taken at 20 °C, in part for experimental convenience. This, in particular, relates to available temperature range of the stopped-flow apparatus. However, the likely stability of partially separated DNA substrates at higher temperatures is also important. An initial test of how the rate of the helicase changes with temperature was done using a steady-state ATPase assay in the presence of three-way junctions. The rate doubled from 20 to 37 °C, and the van't Hoff plot was linear from 10 to 50 °C (data not shown).

In the absence of DNA, the steady-state ATPase rate is $\sim$0.1 s^{-1}, compared to a rate of 7.5 s^{-1} in the presence of a three-way junction. The rate was not accelerated by the presence of 100 nM dT_{30}. At 50 nM blunt-end duplex oligonucleotide (40 bases long), the rate was 0.5 s^{-1}. These DNA concentrations are well above saturating concentrations, if three-way or two-way junctions are used to activate the ATPase activity.

To understand the mechanism of dsDNA unwinding, a kinetic analysis of the reaction catalyzed by the RecG helicase was carried out using a fluorometric assay. The assay was based on the process of static or contact quenching of the fluorescence of a fluorophore by a nonfluorescent dye in its proximity. Figure 1B shows a schematic representation of the labeled three-way DNA junction substrate. A fluoro-

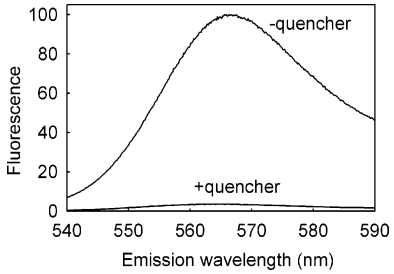

FIGURE 2: Fluorescence emission spectra of oligonucleotide A40 labeled with Cy3 at the 5′-end in buffer A at 20 °C. The oligonucleotide as a single strand (in the absence of quencher) and after the annealing with the oligonucleotide C19 labeled with Dabcyl at the 3′-end. The excitation wavelength was 515 nm.

phore (F) and a quencher (Q) are attached to the 5′- and 3′-ends, respectively, of the duplex lagging arm of the DNA substrate. The signal emitted from the fluorophore upon excitation is quenched due to the presence of the quencher immediately adjacent. A consequence of the unwinding reaction by RecG is that the two strands are separated and the emission signal from the fluorophore is expected to increase.

Different interactive fluorophores (donor−acceptor) or fluorophore−quencher pairs (TAMRA−TAMRA, TAMRA−Dabcyl, Cy3−Cy5, Cy3−Black Hole Quencher 2, and Cy3−Dabcyl) were covalently attached to the ends of the oligonucleotides, as in Figure 1B, to determine the best pair for studying the kinetic mechanism of the ATP-dependent translocation and unwinding. The best combination of quenching efficiency and emission signal change produced during unwinding was obtained using Cy3 and Dabcyl as the fluorophore and quencher, respectively. Dabcyl (Db) is a nonfluorescent quencher that efficiently suppresses the fluorescence of different fluorophores by contact quenching, although it has little spectral overlap with the emission spectra of Cy3 (*28*−*30*). Figure 2 shows the Cy3 fluorescence emission spectra of a Cy3-labeled two-way DNA junction and a doubly labeled Cy3−Dabcyl three-way DNA junction. Cy3 fluorescence is efficiently quenched in the three-way DNA substrates.

Single-turnover kinetic studies of DNA unwinding were performed as described in Experimental Procedures. Briefly, a doubly labeled (Cy3−Dabcyl pair) or a single Cy3-labeled three-way DNA junction was preincubated with excess RecG protein to ensure the RecG·DNA complex was fully formed. This complex was then rapidly mixed with ATP to initiate strand separation, and the fluorescence was followed with time.

Figure 3A shows the results with an A40(Cy3)−B40−C19(Db) junction, which has a 19 bp duplex arm to unwind. The time course shows a distinct lag phase, followed by an increase in fluorescence. The lag is likely to be due to the movement of RecG along the DNA, before reaching a stage where it affects the fluorophore. There is then a fluorescence increase as the fluorophore separates from the quencher followed by a small decrease. Finally, there is a very slow increase in fluorescence, but this was outside the likely time scale of unwinding and so was not used in the analysis; we will return to this phase later.

The same type of measurement was carried out with the A40(Db)−B40−C19(Cy3) junction (Figure 3A). In this case, Cy3 is attached to the 3′-end and Dabcyl to the 5′-end of the duplex lagging arm. The duration of the initial lag phase

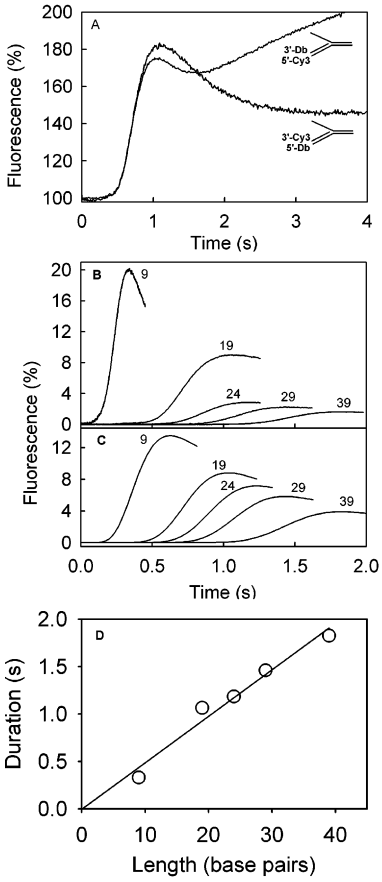

FIGURE 3: Cy3 fluorescence time courses for single-turnover RecG-catalyzed DNA unwinding using differently labeled DNA substrates. (A) Cy3 fluorescence was recorded after rapid mixing with ATP of the preformed complex between 30 nM RecG and 60 nM doubly labeled DNA substrates: A40(Cy3)−B40−C19(Db) with the fluorophore Cy3 attached to the 5′-end and the quencher Dabcyl attached to the 3′-end of the duplex lagging arm and A40(Db)−B40−C19(Cy3) with Cy3 attached to the 3′-end and Dabcyl to the 5′-end. (B) Time courses of the single-turnover kinetic curves for three-way DNA junctions, differing in the number of base pairs in the duplex lagging arm of the DNA substrates. RecG helicase (60 nM) was incubated with 30 nM DNA substrates: A30(Cy3)−B40−C9(Db), A40(Cy3)−B40−C19(Db), A45(Cy3)−B40−C24(Db), A50(Cy3)−B40−C29(Db), and A60(Cy3)−B40−C39(Db). Curves are labeled with the length of oligonucleotide C. Final concentrations were as follows: 60 nM RecG, 30 nM DNA, and 200 μM ATP. (C) Modeled curves, obtained using the kinetic scheme in Figure 4 and the rate constants in Table 1. (D) Amplitudes of the unwinding reaction in panel B (measured as time to maximum fluorescence) are plotted as a function of duplex lagging arm length. The best fit line has a slope of 20.5 s^{-1} and intercept with the length axis of 0.7 (±2.6) base; this is not significantly different from zero.

and the rate during translocation were the same as with the previous substrate. After the increase in Cy3 fluorescence, there is a monoexponential decrease, similar to that obtained before, but then the fluorescence remains fairly constant. The signals observed from these measurements are likely to be mainly due to strand (and therefore fluorophore−quencher) separation. However, other processes such as the proximity of the protein to the fluorophore may contribute to the signals.

RecG-Catalyzed DNA Unwinding as a Function of Lagging Arm Length. To address the kinetics of the dsDNA unwinding by the RecG helicase and the processivity of the reaction, we examined the effect of changing the length of the duplex lagging arm on the single-turnover kinetics (Figure

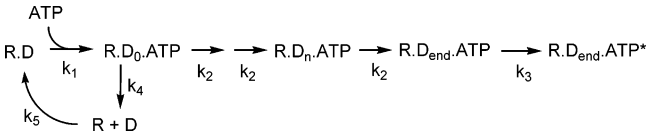

FIGURE 4: Kinetic scheme used in modeling the RecG translocation. All steps were assumed to be irreversible. R is RecG, and D is the DNA junction. D_0, D_n, and D_{end} refer to the position that RecG has reached in strand separation of the lagging arm (no separation, part way, and complete, respectively).

3B). The rest of the DNA junction was unchanged among this range of junctions. The extent of the lag increases with an increase in length, in agreement with the idea that the helicase unwinds by a multistep process with the transient formation of partially unwound DNA intermediates (*9*, *31*). There is a decrease in the amplitude of the fluorescence change as the length of the duplex lagging arm increases. This decrease may be due in part to the multistep nature of RecG unwinding and in part due to partial dissociation of RecG. The modeling of the multistep process (below) shows this decrease at least qualitatively.

The relationship between the length of the duplex lagging arm and the duration of translocation of RecG along the duplex allows determination of the translocation rate. This was dealt with in two ways, first by a simple determination of the time shift in fluorescence curves as a function of length and second by modeling the kinetic reaction. The time taken to reach the maximum fluorescence was used as a measure of the duration of unwinding. There is an approximately linear increase in this time with length (Figure 3C), and the slope suggests that the protein moves at a rate of 20.5 bp s^{-1} along the duplex lagging arm during the unwinding process.

Quantitative Analysis of the DNA Unwinding Time Courses. These kinetic data using different length arms were modeled using the simple kinetic scheme for the translocation depicted in Figure 4. In this model, there is an initial conformation change, possibly due to a conformational change on binding ATP, which configures the enzyme for the unwinding. A series of identical translocation steps follows this, each having the same rate constant that is independent of the length of the dsDNA. In this model, the number of kinetic translocation steps is set equal to the number of bases in the duplex lagging arm. At each step, RecG and the lagging arm can dissociate and then rebinding occurs at the start. Finally, the protein reaches the end of the double strand, and the complex undergoes a conformation change, which is undefined but allows the decrease in fluorescence to be accommodated.

In practice, there are several reasons why the reaction may be more complex than this model, and these will be discussed later. In addition, differences in fluorescence amplitudes with a change in DNA length could not be well fitted with a single set of rate constants. A best fitting set of rate constants was obtained for the set of curves in Figure 3B, and the resulting, modeled curves are in Figure 3D. These fit well the relative changes with time, and the rate constants are listed in Table 1. The translocation rate from this modeling is slightly faster than that obtained from the slope of Figure 3C.

ATPase Activity during Translocation. The amount of ATP hydrolyzed by RecG during translocation and unwinding was

Table 1: Kinetic Parameters Obtained from Modeling the Unwinding of Duplex Lagging Arm DNA by RecG Helicase[a]

rate constant	value (s^{-1})	event
k_1	7	conformational change on binding ATP
k_2	26	translocation step of one base
k_3	3.0	conformational change after reaching the end of the duplex
k_4	0.98	dissociation at each step
k_5	10	rebinding to the DNA junction

[a] The steps refer to the reaction scheme in Figure 4.

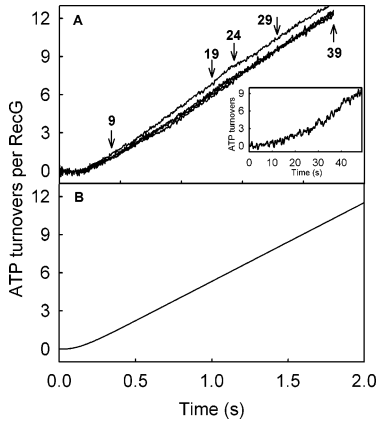

FIGURE 5: Kinetics of release of P_i after premixing of RecG with DNA substrates with duplex lagging arms that differ in length. (A) ATPase activity was measured by linking ATP hydrolysis to the change in fluorescence observed in the P_i sensor MDCC-PBP. Each curve is the average of four single measurements. Arrows indicate the time for the duration of the translocation for each length, identical to times in Figure 3D. The inset shows a trace for A45−B40−C24 in which the DNA junction and RecG were not premixed: DNA with ATP was mixed in the stopped-flow apparatus with RecG at the same final concentrations described above. (B) Theoretical curve modeled using the reaction scheme in Figure 4 and rate constants listed in Table 1. It was assumed that P_i is released every third translocation step. The slope is 6.2 s^{-1}.

measured with a P_i sensor, a fluorescent coumarin-labeled phosphate binding protein (MDCC-PBP) (*21*). The RecG−junction complex was rapidly mixed with ATP in the presence of the sensor (Figure 5). The presence of three-way DNA junctions with a duplex lagging arm of different lengths resulted in a large activation of the ATPase activity relative to that of RecG alone. After an initial lag, there is ATP hydrolysis at an approximately constant rate of 7.6 s^{-1}, and this is multiturnover in terms of RecG. This constant rate continues after the time expected for complete unwinding of the DNA substrate. The shape of the curve is independent of the length of the RecG arm.

This suggests either that RecG stalls after reaching the end of the duplex lagging arm of the DNA substrate but continues to hydrolyze ATP at a similar rate or that it rebinds rapidly to a new DNA junction for a further cycle of unwinding. However, a similar measurement of ATPase activity in which RecG is not prebound to DNA gives a much slower rate (Figure 5A). Here, the rate is likely to be limited by very slow binding of RecG to DNA and/or some conformation change to produce a productive complex. An independent measurement of the rate of binding of RecG to a junction (below) also suggests this binding is slow. We therefore conclude that RecG remains bound to the junction after the completion of the strand separation and that the

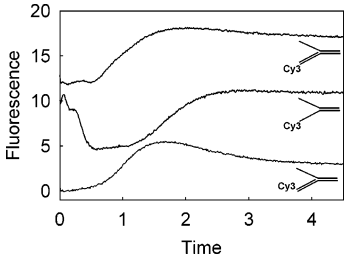

FIGURE 6: Cy3 fluorescence time courses for single-turnover RecG-catalyzed DNA unwinding using differently labeled DNA substrates. Each curve is offset by 5%. The top curve is for A40(Cy3)−B40−C19 with the fluorophore Cy3 attached to the 5′-end. The middle curve is for A40(Cy3)−B40 with the fluorophore Cy3 attached to the 5′-end. The bottom curve is for A40−B40−C19(Cy3) with the fluorophore Cy3 attached to the 3′-end. Final concentrations were as follows: 60 nM RecG, 30 nM DNA, and 200 μM ATP.

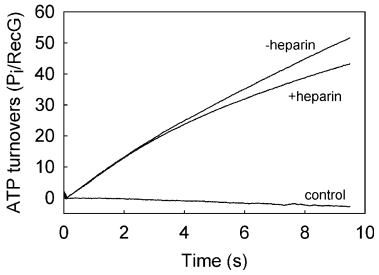

FIGURE 7: Kinetics of release of P_i during interaction of RecG with the three-way DNA substrate A40−B40−C19 in the absence and the presence of heparin. RecG was premixed with the DNA substrate and then mixed with ATP in the absence or presence of heparin. In the control, RecG was premixed with heparin and then mixed with ATP and DNA. Final concentrations were as follows: 5 nM RecG, 100 nM DNA, 200 μM ATP, and 2 mg/mL heparin.

ATPase rate continues at the same rate. This idea is supported by measurement of the ATP hydrolysis by a two-way junction, which would be the initial product from unwinding the three-way junction (see below).

The ATPase reaction was modeled using the rate constants for the scheme in Figure 4 that best fit the Cy3 data (Table 1). The curve is shown in Figure 5B and shows a slope of 6.2 s^{-1}, ~20% slower than the observed slope. However, this difference is greatly reduced with the modeled rate at 6.8 s^{-1}, if the dissociation at each step is reduced to zero.

Activity of RecG with a Two-Way Junction. To characterize the ability of RecG to function with single-strand leading and lagging arms, measurements were carried out using two-way DNA junctions. To provide a direct comparison, measurements were also carried out with three-way junctions that were labeled only with a single Cy3 on different strands of the lagging arm (Figure 6). This also allowed a direct assessment of the extent of direct interactions with the RecG protein on the Cy3 fluorescence. As expected due to the absence of quenching, the initial fluorescence is higher than in the Cy3−Dabcyl DNA substrates. The time course obtained using the substrate labeled at the 3′-end, A40−B40−C19(Cy3), shows a lag phase and an increment in fluorescence, followed by a monoexponential decrease. In this case, a fluorescence change occurs when the protein is near the fluorophore. Note that the rates are somewhat slower than with the Cy3−Dabcyl DNA: this may reflect the contribution of an all or nothing signal change with the latter. With the three-way DNA substrate A40(Cy3)−B40−C19, labeled at the 5′-end, there was a lag phase followed by an increase with a constant rate similar to that observed with the DNA substrate A40−B40−C19(Cy3).

The two-way DNA junction A40(Cy3)−B40 with a single-stranded lagging arm gave a somewhat different fluorescence time course. Immediately after the mixing with ATP, there is a complex decrease in fluorescence for ~0.5 s, followed by a lag phase and then an increase. Finally, there is a small decrease in Cy3 fluorescence. The initial phase is presumably due to the process before unwinding begins that does not occur with the more natural three-way DNA junction substrate. This may be some rearrangement of the RecG binding to DNA. The lag phase and increase in fluorescence observed were almost the same as with the three-way DNA junctions labeled and suggest that, apart from the initial phase, the lagging arm of the two-way junction is translocated with similar kinetics to the three-way junction.

A measurement of ATPase activity of the two-way DNA junctions gave similar curves to those for three-way junctions (Figure 5). When the junction was prebound with RecG, there is a lag (~100 ms) followed by a linear reaction at 7.0 s^{-1} (data not shown).

RecG Remains Bound to the Junction after Translocation. As described in the introductory section, various helicases have been successfully trapped following their release from DNA by rapid binding to heparin. The protein is thus prevented from rebinding to free DNA. In the case of RecG, this was not successful, and an example is shown in Figure 7. When the preformed RecG−DNA complex was rapidly mixed with ATP and heparin, there is a qualitative difference with the time course obtained in the absence of heparin. However, inhibition of ATPase activity occurs very slowly. If the protein and heparin were premixed before mixing with ATP and DNA, heparin was effective in completely inhibiting the ATPase activity.

When using fluorescent DNA substrates, either heparin or excess unlabeled DNA was added to attempt to trap free RecG. In neither case were the unwinding kinetics perturbed by these additions (data not shown), suggesting that the trapping was unsuccessful. We observed the same initial lag phase and increase in the Cy3 fluorescence when the protein reaches the end of the junction in the presence of the trap.

We therefore conclude that the protein remains bound to the junction at the end of the initial translocation and that dissociation occurs only very slowly, while ATPase activity continues. This is in agreement with the lack of a break in the ATPase traces in Figure 5.

RecG−DNA Binding. To gain an idea of binding kinetics and affinity for RecG with DNA, a three-way DNA junction was used with an only 10 bp duplex length in the template arm and Cy3 at the 5′-end of the template arm, as described in Experimental Procedures. This gives a small increase in fluorescence on binding RecG, although ATPase activity measurements with this substrate indicate that a longer template arm is required for translocation. Measurements were taken as described in Experimental Procedures in the absence of ATP. Binding traces were fitted to a double exponential, yielding two constant rates: 100 and 6 s^{-1} with similar amplitudes (data not shown). The rates did not vary significantly within the concentration range that was studied. Dissociation traces gave a single rate of 0.13 s^{-1}. A titration of RecG into the DNA solution gave an increase in fluorescence with a K_d of 20 nM (data not shown). The

complex curves of the binding kinetics did not allow a full analysis of these data. However, it is clear that RecG binds tightly to this junction, and dissociation in the absence of ATP is slow on the time scale of translocation. This confirms that the DNA−protein complex is likely to be fully formed under the conditions of the ATPase activity and translocation measurements described above.

DISCUSSION

The data presented here provide a quantitative analysis of the kinetics of dsDNA unwinding by the *T. maritima* RecG helicase. Translocation and ATPase activity have been followed in real time.

Translocation Measurements. In the three-way DNA unwinding reaction catalyzed by RecG (Figure 3), the Cy3 fluorescence time course exhibits a lag phase, followed by a fluorescence increase. The initial part of this lag (~0.1 s) is likely to be equivalent to that in the ATP hydrolysis measurements (Figure 5). This is possibly an ATP-driven change to give the active conformation of the RecG·DNA complex before cycles of ATP hydrolysis and translocation begin. A similar lag was seen in the PcrA translocation measurements on single-stranded DNA (*32*). However, the rest of this lag phase in the Cy3−Dabcyl measurements is likely to be due to the time taken for multiple translocation steps prior to separation of Cy3 from its quencher when RecG unwinds to the end of the lagging arm. The time taken for the lag phase increases with the length of the duplex lagging arm, in agreement with the idea that this phase and subsequent fluorescence increase are associated with multistep translocation.

If the helicase dissociates before complete separation of the duplex DNA, partially unwound DNA molecules may be formed. These intermediates could reanneal to form the duplex DNA substrate, resulting in no change in the fluorescence signal for that molecule. Under the conditions of the experiment, RecG would rebind to DNA and restart unwinding. These processes are included in our modeling, although as described later they are not considered significant.

The lag phase is followed by an increase in fluorescence due to the release of the Cy3-labeled strand from the unwound Dabcyl-labeled strand. However, it is likely that this increase in fluorescence has contributions from several other causes. Most importantly, there are several pieces of evidence that RecG does not dissociate fully from the DNA after the unwinding reaction (we will discuss this later). Second, it is clear that Cy3 fluorescence is directly affected by RecG, for example, in Figure 6: when RecG reaches Cy3, the intensity of the fluorophore increases presumably due to direct interactions with the protein, for example, as shown previously with another helicase (*19*). This in turn provides a route for explaining the difference in traces depending on whether the Cy3 and Dabcyl are bound on the 5′- and 3′-ends, respectively, or whether they are reversed (Figure 3A). The protein could remain interacting with the end of the arm, and a possible conformational change before dissociation from the DNA could vary the effect of the protein on fluorescence. When Cy3 is on the 3′-end, it is most likely that this strand dissociates after some relaxation so that the Cy3 becomes unaffected by the RecG.

The amplitude of this fluorescence increase after the lag decreases as the length of the duplex lagging arm increases. Such a decrease is expected for a multistep process as shown in the modeling in Figure 3C: as the number of steps increases, the distribution of RecG along the DNA broadens, as the population of protein undergoes more discreet steps. Other effects may contribute to this decrease. Premature dissociation of RecG from this arm will be more significant as the length increases, if limited processivity is a factor. As the apparent translocation time increases approximately linearly with time (Figure 3C), this suggests that for the lengths of DNA studied, processivity is large. However, even a small rate of dissociation assumed in the modeling produces a significant decrease in amplitude with length, while only slightly affecting the position of the fluorescence maximum. Nevertheless, these factors do not fully explain the changes in amplitude with length, and we will return to this later, particularly with respect to the relation between our kinetic data and structural aspects of the helicase−DNA complex and the idea that RecG does not simply dissociate after unwinding.

Otherwise, the lag phases and rise times in Figure 3B are reasonably modeled by a single set of rate constants. The shortest arm (9 bp) is an apparent exception. Not only is the relative amplitude large, the time of the maximum fluorescence was not modeled well. This may be because such a short arm length is partially frayed before ATP-driven unwinding starts, or because the interactions with RecG occur along the full length of this arm; i.e., the arm is shorter than its RecG binding site. This short length could allow some interaction of RecG with Cy3 from zero time.

Figure 3C shows that the time to reach the fluorescence maximum linearly increases with oligonucleotide length. Extrapolation back to zero time is at 0.7 (±2.6) base. This suggests that the number of bases translocated is similar to or slightly less than the actual length. Such a difference between translocation length and actual length could arise from the fact that the protein binding site requires several bases of single-stranded DNA for tight binding. This could affect either the initial point of translocation or the end of the process. Examination of the crystal structure of RecG (*20*) suggests there are one or two unpaired bases between the duplex template strand and the duplex lagging strand. Our substrates have one base here. Thus, it is unlikely that the initial binding of RecG to DNA requires significant duplex separation. Toward the end of the translocation there could be spontaneous separation of the end of the lagging strand, also leading to a difference between actual duplex length and the number of bases that need to be translocated. The relatively low temperature used in these measurements makes this possibility less likely, and Figure 3C suggests that it is not a major factor. Indeed, the experimental design may also minimize spontaneous unwinding, as the Cy3−quencher interaction may stabilize interaction between bases at the arm end.

On What DNA Structures Does RecG Act? The question of what DNA structures are good substrates for DNA has been addressed previously (*6*, *33*). We have taken some measurements in the context of our junction experiments. Steady-state measurements suggest that there is low ATPase activity in the absence of DNA. Single-stranded and blunt-end duplex DNA do not activate RecG or possibly bind only

weakly to the protein. This in turn suggests that in our measurements, productive complexes with the three-way junctions occur only when RecG binds actually at the arm junction.

Furthermore, evidence can be gleaned that separation of the lagging arm is the main or only activity. Figure 3C indicates that the length of this arm is the main determinant in the time of the fluorescence increase. As indicated earlier, similar but smaller fluorescence changes were observed with Cy3 alone at the end of the lagging arm. However, Cy3 at the end of the template arm gave only a very small signal on this time scale (data not shown), suggesting that this arm is left intact.

Step Size. For the longer DNA substrates, the translocation rate constant from the modeling is 26 s^{-1}, in contrast with the ATP hydrolysis rate of 7.6 s^{-1}. This implies a movement of ~3 bp per ATP for the types of DNA used in our study. RecG, as a SF-2 helicase and as suggested by its crystal structure, probably drives movement via interaction with a fully duplex template arm, rather than via interaction with single strands. This is different from those superfamily-1 helicases that often have a step size of 1 bp per ATP. An example is PcrA, in which detailed interactions with bases change during the ATPase cycle, and impose a single-base step size (*34*, *35*). Interaction of RecG with the surface of the duplex must allow translocation. Both this and the larger potential conformation changes may enable the larger step during each ATPase cycle.

The RecG used is from a thermophile, so its natural temperature is above that experimentally readily accessible with these types of substrates and methods. The linear van't Hoff relationship between the steady-state ATPase rate and temperature does not give evidence for any major change as the temperature increases, apart from a typical rate increase. It is possible that spontaneous melting of the duplex is significant at high temperatures, and this could potentially modify the efficiency. It is likely that there is a precise relationship between ATPase-driven conformation changes and step size, so it seems unlikely that this measure would change with temperature.

An important corollary is the implication of this result in terms of possible numbers of kinetic steps. The modeling is better when the number of kinetic steps approximately equals the number of bases. Using the number of kinetic steps equal to the number of ATP molecules hydrolyzed did not produce such a good fit, as the observed shape of the fluorescence traces could not be reproduced. This difference may be due to limitations of the model, which is all or nothing; i.e., the fluorescence increase occurs solely on the final step of strand separation. In fact, the total fluorescence change arises due to other effects apart from physical separation of the quencher from Cy3, and these may be operating over the movement of several bases prior to final strand separation. This in turn may affect the observed shape of the fluorescence curves.

However, the modeling may point to each ATP hydrolysis cycle being divided into substeps. In practice, the modeling could not distinguish between identical substeps and substeps of different but similar rate constants. Indeed, a model with two substeps of movement in each ATPase cycle would improve on the curve shape over single steps. Such multistep movement has been observed for some, but certainly not all, myosins. In those cases, there is evidence that at least two distinct and separate movements of the protein occur during the ATPase cycle. These movements are associated with P_i and then ADP release steps (*36*, *37*). Our experiments were performed at saturating ATP concentrations, and the modeling does not include any steps related to ATP binding, hydrolysis, or release of ADP, P_i, and any associated conformational changes. However, these may be the basis for such substeps during the ATPase cycle. Further analysis of this aspect may require more data on the ATPase cycle itself, but also specifically on associated structural changes.

RecG Remains Attached to DNA after Translocation. Several pieces of evidence suggest that RecG remains associated with the DNA after the initial translocation and unwinding. First and most directly, trapping methods that work with other helicases that are free in solution are ineffective at sequestering RecG after unwinding. However, heparin does bind to free RecG in the absence of junction and prevents it from functioning. Second, there is no break in the ATPase traces at times expected for complete unwinding. As the two-way junction has ATPase activity similar to that of the three-way junction, it is likely that the protein remains attached to the junction after it changes from three-way to two-way. Finally, the Cy3 fluorescence is affected by the presence of RecG for many seconds after the initial translocation reaction is complete. It is likely that dissociation is very slow and suggests that strong interactions between the DNA and RecG remain.

Potential Need To Extend the Modeling. We have chosen to deal with our data through a simple kinetic scheme in Figure 4, in which each step results in translocation of one base and each of these steps has the same rate constant. This models well the time of the fluorescence increase, but not the change in fluorescence amplitudes with length. A rapid drop in amplitude is observed as the arm length increases to 24 bp: after that the changes are much smaller. In addition, the trace obtained with a very short (9 bp) duplex arm is not well modeled: this requires a faster translocation rate.

We will now examine how the structure of the RecG·DNA junction complex may impose a more complex mechanism. This includes the DNA structure per se and the interactions between RecG and DNA. Each unwinding rate constant may depend on both base composition and sequence, but an assumption about the constant rate seems justified because our DNA substrates have the same structure and a G-C content of ~45% so that minor variations along each length would not be resolved. McGlynn and Lloyd (*6*) used different fork substrates for RecG in which the leading and lagging strand arm lengths were varied. The highest activity was for substrates in which the lengths of the arms were similar. In addition, our junctions are made with noncomplementary leading and lagging arms, and the length of the leading arm is a constant 20 bases. This is a practical factor so that the junctions can be purified and are stable.

Now consider the lengths of each arm that may interact with the protein at any time, based on the published crystal structure (*5*). The crystal structure had a 10 bp template arm, but possibly up to ~20 bp in this arm may all interact with the protein. Somewhat fewer than 10 bp on the lagging arm may interact. The structure has no duplex in the leading arm and suggests there is little scope for much interaction with duplex here. In vivo, leading and lagging arms are complementary, and as their second strands are stripped off, new

duplex presumably form and displaces the previous section of template duplex. With our substrates, we can consider several phases in terms of the structure of DNA associated with RecG.

During translocation of the first 20 bases, two strands (one lagging, one leading), albeit noncomplementary, are being pulled into the RecG surface. In principle, this may displace the template duplex arm or form some sort of loop structure, leaving the duplex template strand in position. After that, only one strand (lagging arm) is being translocated. The final ~10 bp of the lagging arm duplex is translocated while fully interacting with RecG. It may be that these different phases of the overall translocation are governed by rate constants that are not exactly the same, in terms of both translocation and dissociation. Thus, it will be important to extend this work to junctions having complementary leading and lagging arms as well as to try to observe gross movement of RecG relative to the various ends of a junction.

Some helicases function less efficiently and with reduced processivity when separated from the molecular machinery and coupling factors with which they associate and operate in vivo. This is because the function of helicases within such assemblies is not only to catalyze the opening of a dsDNA segment but also to drive rearrangements in which one or both of the ssDNA products end up bound to another macromolecular component. Often, the inclusion of loading or trapping factors within the reaction assay mixture can improve helicase activity (*14*, *19*, *22*, *38*). However, such components may also modify aspects of the molecular mechanisms of the helicase from those displayed in isolation, or when the helicase is properly coupled within the relevant macromolecular machine (*39*).

This work provides a picture of the mechanism of RecG unwinding to complement that of the known crystal structure (*5*). The complex movement of DNA relative to the protein is a direct consequence of the function of RecG. The step size of 3 bp per ATP imposes a higher thermodynamic efficiency than the helicases with a step size of 1. However, for natural three-way junctions with complementary leading and lagging arms, there is no net separation of the duplex. It will be of interest to see whether the translocation rate, step size, and processivity change with different types of DNA substrate.

ACKNOWLEDGMENT

We thank Mrs. Jackie Hunter (NIMR, London, U.K.) for preparing the phosphate sensor, Mark S. Dillingham (University of Bristol, Bristol, U.K.) for advice and support, Martin R. Singleton (Cancer Research UK) for helping to design the preparation of the three-way DNA substrates, and Dale B. Wigley (Cancer Research UK) for kindly providing the RecG expression system and for communicating and discussing data in advance of publication.

REFERENCES

1. Singleton, M. R., and Wigley, D. B. (2002) Modularity and specialization in superfamily 1 and 2 helicases, *J. Bacteriol. 184*, 1819−1826.
2. Tuteja, N., and Tuteja, R. (2004) Prokaryotic and eukaryotic DNA helicases: Essential molecular motors for cellular machinery, *Eur. J. Biochem. 271*, 1835−1848.
3. McGlynn, P., and Lloyd, R. G. (2000) Modulation of RNA polymerase by (p)ppGpp reveals a RecG-dependent mechanism for replication fork progression, *Cell 101*, 35−45.
4. McGlynn, P., Lloyd, R. G., and Marians, K. J. (2001) Formation of Holliday junctions by regression of nascent DNA in intermediates containing stalled replication forks: recG stimulates regression even when the DNA is negatively supercoiled, *Proc. Natl. Acad. Sci. U.S.A. 98*, 8235−8240.
5. Singleton, M. R., Scaife, S., and Wigley, D. B. (2001) Structural analysis of DNA replication fork reversal by RecG, *Cell 107*, 79−89.
6. McGlynn, P., and Lloyd, R. G. (2001) Rescue of stalled replication forks by recG: Simultaneous translocation on the leading and lagging strand templates supports an active DNA unwinding model of fork reversal and Holliday junction formation, *Proc. Natl. Acad. Sci. U.S.A. 98*, 8227−8234.
7. Briggs, G. S., Mahdi, A. A., Wen, Q., and Lloyd, R. G. (2005) DNA Binding by the Substrate Specificity (Wedge) Domain of RecG Helicase Suggests a Role in Processivity, *J. Biol. Chem. 280*, 13921−13927.
8. Whitby, M. C., and Lloyd, R. G. (1998) Targeting Holliday junctions by the RecG branch migration protein of *Escherichia coli*, *J. Biol. Chem. 273*, 19729−19739.
9. Ali, J. A., and Lohman, T. M. (1997) Kinetic measurement of the step size of DNA unwinding by *Escherichia coli* UvrD helicase, *Science 275*, 377−380.
10. Ali, J. A., Maluf, N. K., and Lohman, T. M. (1999) An oligomeric form of *E. coli* UvrD is required for optimal helicase activity, *J. Mol. Biol. 293*, 815−833.
11. Jankowsky, E., Gross, C. H., Shuman, S., and Pyle, A. M. (2000) The DExH protein NPH-II is a processive and directional motor for unwinding RNA, *Nature 403*, 447−451.
12. Lucius, A. L., Vindigni, A., Gregorian, R., Ali, J. A., Taylor, A. F., Smith, G. R., and Lohman, T. M. (2002) DNA unwinding step-size of *E. coli* RecBCD helicase determined from single turnover chemical quenched-flow kinetic studies, *J. Mol. Biol. 324*, 409−428.
13. Galletto, R., Jezewska, M. J., and Bujalowski, W. (2004) Unzipping mechanism of the double-stranded DNA unwinding by a hexameric helicase: Quantitative analysis of the rate of the dsDNA unwinding, processivity and kinetic step-size of the *Escherichia coli* DnaB helicase using rapid quench-flow method, *J. Mol. Biol. 343*, 83−89.
14. Jeong, Y. J., Levin, M. K., and Patel, S. S. (2004) The DNA-unwinding mechanism of the ring helicase of bacteriophage T7, *Proc. Natl. Acad. Sci. U.S.A. 101*, 7264−7269.
15. Levin, M. K., Wang, Y. H., and Patel, S. S. (2004) The functional interaction of the hepatitis C virus helicase molecules is responsible for unwinding processivity, *J. Biol. Chem. 279*, 26005−26012.
16. Bjornson, K. P., Amaratunga, M., Moore, K. J., and Lohman, T. M. (1994) Single-turnover kinetics of helicase-catalyzed DNA unwinding monitored continuously by fluorescence energy transfer, *Biochemistry 33*, 14306−14316.
17. Houston, P., and Kodadek, T. (1994) Spectrophotometric assay for enzyme-mediated unwinding of double-stranded DNA, *Proc. Natl. Acad. Sci. U.S.A. 91*, 5471−5474.
18. Cheng, W., Hsieh, J., Brendza, K. M., and Lohman, T. M. (2001) *E. coli* Rep oligomers are required to initiate DNA unwinding *in vitro*, *J. Mol. Biol. 310*, 327−350.
19. Lucius, A. L., Wong, C. J., and Lohman, T. M. (2004) Fluorescence stopped-flow studies of single turnover kinetics of *E. coli* RecBCD helicase-catalyzed DNA unwinding, *J. Mol. Biol. 339*, 731−750.
20. Choudhary, S., Sommers, J. A., and Brosh, R. M., Jr. (2004) Biochemical and kinetic characterization of the DNA helicase and exonuclease activities of Werner syndrome protein, *J. Biol. Chem. 279*, 34603−34613.
21. Brune, M., Hunter, J. L., Howell, S. A., Martin, S. R., Hazlett, T. L., Corrie, J. E. T., and Webb, M. R. (1998) Mechanism of inorganic phosphate interaction with phosphate binding protein from *Escherichia coli*, *Biochemistry 37*, 10370−10380.
22. Fischer, C. J., Maluf, N. K., and Lohman, T. M. (2004) Mechanism of ATP-dependent translocation of *E. coli* UvrD monomers along single-stranded DNA, *J. Mol. Biol. 344*, 1287−1309.
23. Bianco, P. R., and Kowalczykowski, S. C. (2000) Translocation step size and mechanism of the RecBC DNA helicase, *Nature 405*, 368−372.

24. Paolini, C., De Francesco, R., and Gallinari, P. (2000) Enzymatic properties of hepatitis C virus NS3-associated helicase, *J. Gen. Virol. 81*, 1335−1345.
25. Webb, M. R. (2003) A fluorescent sensor to assay inorganic phosphate, in *Kinetic analysis: A practical approach* (Johnson, K. A., Ed.) pp 131−152, Oxford University Press, Oxford, U.K.
26. Gasteiger, E., Gattiker, A., Hoogland, C., Ivanyi, I., Appel, R. D., and Bairoch, A. (2003) ExPASy: The proteomics server for in-depth protein knowledge and analysis, *Nucleic Acids Res. 31*, 3784−3788.
27. Leatherbarrow, R. J. (2001) *Grafit*, version 5, Erithacus Software Ltd., Horley, U.K.
28. Tyagi, S., and Kramer, F. R. (1996) Molecular beacons: Probes that fluoresce upon hybridization, *Nat. Biotechnol. 14*, 303−308.
29. Tyagi, S., Bratu, D. P., and Kramer, F. R. (1998) Multicolor molecular beacons for allele discrimination, *Nat. Biotechnol. 16*, 49−53.
30. Marras, S. A., Kramer, F. R., and Tyagi, S. (2002) Efficiencies of fluorescence resonance energy transfer and contact-mediated quenching in oligonucleotide probes, *Nucleic Acids Res. 30*, e122.
31. Yodh, J. G., and Bryant, F. R. (1993) Kinetics of ATP hydrolysis during the DNA helicase II-promoted unwinding of duplex DNA, *Biochemistry 32*, 7765−7771.
32. Dillingham, M. S., Wigley, D. B., and Webb, M. R. (2000) Demonstration of unidirectional single-stranded DNA translocation by pcrA helicase: Measurement of step size and translocation speed, *Biochemistry 39*, 205−212.
33. Mahdi, A., McGlynn, P., Levett, S., and Lloyd, R. (1997) DNA binding and helicase domains of the *Escherichia coli* recombination protein RecG, *Nucleic Acids Res. 25*, 3875−3880.
34. Soultanas, P., Dillingham, M., Wiley, P., Webb, M. R., and Wigley, D. B. (2000) Uncoupling DNA translocation and helicase activity in pcrA: Direct evidence for an active mechanism, *EMBO J. 19*, 3799−3810.
35. Velankar, S. S., Soultanas, P., Dillingham, M. S., Subramanya, H. S., and Wigley, D. B. (1999) Crystal structures of complexes of pcrA DNA helicase with a DNA substrate indicate an inchworm mechanism, *Cell 97*, 75−84.
36. Veigel, C., Coluccio, L. M., Jontes, J. D., Sparrow, J. C., Milligan, R. A., and Molloy, J. E. (1999) The motor protein myosin-I produces its working stroke in two steps, *Nature 398*, 530−533.
37. Whittaker, M., Wilson-Kubalek, E. M., Smith, J. E., Faust, L., Milligan, R. A., and Sweeney, H. L. (1995) A 35-Å movement of smooth muscle myosin on ADP release, *Nature 378*, 748−751.
38. Roman, L. J., and Kowalczykowski, S. C. (1989) Characterization of the helicase activity of the *Escherichia coli* RecBCD enzyme using a novel helicase assay, *Biochemistry 28*, 2863−2873.
39. von Hippel, P. H., and Delagoutte, E. (2001) A general model for nucleic acid helicases and their "coupling" within macromolecular machines, *Cell 104*, 177−190.

BI0512851